fractal and fractional

Article

Synchronization of Incommensurate Fractional-Order Chaotic Systems Based on Linear Feedback Control

Fei Qi [1], Jianfeng Qu [1,*], Yi Chai [1], Liping Chen [2] and António M. Lopes [3]

[1] School of Automation, Chongqing University, Chongqing 400044, China; cquqifei@163.com (F.Q.); chaiyi@cqu.edu.cn (Y.C.)
[2] School of Electrical Engineering and Automation, Hefei University of Technology, Hefei 230009, China; lip_chenhut@126.com
[3] LAETA/INEGI, Faculty of Engineering, University of Porto, Rua Dr. Roberto Frias, 4200-465 Porto, Portugal; aml@fe.up.pt
* Correspondence: qujianfeng@cqu.edu.cn

Abstract: The dynamics and synchronization of fractional-order (FO) chaotic systems have received much attention in recent years. However, the research are focused mostly on FO commensurate systems. This paper addresses the synchronization of incommensurate FO (IFO) chaotic systems. By employing the comparison principle for FO systems with multi-order and the linear feedback control method, a sufficient condition for ensuring the synchronization of IFO chaotic systems is developed in terms of linear matrix inequalities (LMIs). Such synchronization condition relies just on the system parameters, and is easily verify and implemented. Two typical FO chaotic systems, named the IFO Genesio-Tesi system and Hopfied neural networks are selected to demonstrate the effectiveness and feasibility of the proposed method.

Keywords: fractional-order systems; chaos; synchronization; state feedback control

Citation: Qi, F.; Qu, J.; Chai, Y.; Chen, L.; Lopes, A.M. Synchronization of Incommensurate Fractional-Order Chaotic Systems Based on Linear Feedback Control. *Fractal Fract.* **2022**, *6*, 221. https://doi.org/10.3390/fractalfract6040221

Academic Editor: Ivanka Stamova

Received: 3 March 2022
Accepted: 12 April 2022
Published: 14 April 2022

1. Introduction

Fractional calculus and FO systems theory are rapid developing topics in today science and engineering. It has been proven that the integer-order modeling techniques may not yield accurate descriptions for the dynamics of some systems [1,2], especially when memory effects are present. Fractional calculus provides new insights into systems' modeling, and successful cases of its use can be found in control theory, mathematics, economics, mechanics, biology, chemistry, and signal and image processing [3–6].

With the introduction of fractional derivatives, the FO nonlinear systems have revealed their complex dynamic behavior, such as chaos, bifurcations, attractors and multi-stability states [7–9]. Due to their potential applications in many fields, the FO chaotic systems have been extensively studied [10,11]. As a collective behavior, chaos synchronization is one of the most important branches of chaos, and has extensive application in a number of areas, namely secure communication, signal encryption and fault diagnosis [12,13]. Recently, synchronization of FO chaotic systems has attracted great attention, with various control methods being proposed to achieve synchronization, such as active [14], impulsive [15], adaptive [16], fuzzy [17], passive [18], sliding mode [19], and feedback [20] control, among others. Meanwhile, many different types of synchronization of FO chaotic system have been introduced. We can mention complete [21], projective [17,22], and lag [23,24] synchronization, to cite a few.

It should be noted that most of the research efforts mentioned above have focused on commensurate FO chaotic systems, meaning that the fractional derivatives of the states are of identical order. The Matignon's stability theorem and its generalization, and the FO Lyapunov method are two of the most used tools to design synchronization controllers for commensurate FO systems [25,26]. Chaotic behavior not only exists in commensurate

FO systems, but can also be verified in IFO systems. Indeed, we mention, the coexistence of multiple attractors in IFO systems was addressed in [27,28]. Bifurcations in a delayed fractional predator-prey system with incommensurate orders were discussed in [29]. Chaos and coexisting attractors in a glucose-insulin regulatory IFO system were considered in [30]. Compared with commensurate FO chaotic systems, IFO chaotic systems have multiple different orders and unveil more complex dynamics. Therefore, the synchronization of IFO systems has received increasing attention in the last few years. For example, the problem of generalized function projective synchronization of nonlinear uncertain time-delay IFO chaotic systems with input nonlinearities was studied in [31]. A fuzzy adaptive controller for achieving an appropriate generalized projective synchronization of two IFO chaotic systems was proposed in [32]. An observer model free type for synchronization of IFO systems was presented in [33]. A composite learning fuzzy control to synchronize two different uncertain IFO time-varying delayed chaotic systems with unknown external disturbances and mismatched parametric uncertainties via the Takagi-Sugeno fuzzy method was proposed in [34]. Nevertheless, due to the lack of stability of IFO systems, the synchronization of IFO chaotic systems is still in an early stage and has not been fully explored.

In this paper the synchronization of IFO chaotic systems based on linear feedback control is addressed. The main result is the derivation of a simple and economical method for assuring synchronization. To the best of authors knowledge, this control method has not been applied to the problem at hand. The main contributions are: (1) synchronization of IFO chaotic systems, including the irrational-order case is considered; (2) linear state feedback control is used to achieve synchronization; (3) synchronization condition is established in terms of linear matrix inequalities (LMIs).

The paper is organized as follows. Section 2 describes the problem and some lemmas necessary for the method developed. Section 3 presents the main results and discusses the most relevant details. Section 4 demonstrates the effectiveness of the novel control scheme with two numerical examples. Finally, Section 5 outlines the main conclusions.

The following standard notations are used. The symbol I represents the identity matrix with appropriate dimension, the superscript T stands for matrix transpose, the function $\mathrm{diag}(\cdot)$ corresponds to a diagonal matrix, the inequality $X > 0$ (<0) refers to symmetric positive definite (negative definite) matrix, the symbol $\otimes$ is the Kronecker product, the condition $\mathrm{sym}\{X\} = X + X^T$, $R^{p\times q}$ represents the real $p \times q$ matrix set, expression $H_+^{p\times q}$ denotes the real symmetric positive definite $p \times q$ matrix set, and $\oplus_{i=1}^{k} x_i = \mathrm{diag}\{x_1, x_2, \cdots x_n\}$.

2. System Description and Preliminaries

In this section we introduce the problem and some necessary lemmas of fractional calculus or FO systems.

We consider the following IFO chaotic system described by

$$D^{\bar{\alpha}}x = Ax + f(x), \tag{1}$$

where $D^{\bar{\alpha}}x := D^{\bar{\alpha}}x(t) = [D^{\alpha_1}x_1(t), D^{\alpha_2}x_2(t), \cdots, D^{\alpha_n}x_n(t)]^T$, α_i being positive real non-integer numbers. The Caputo derivative of order α of a function $x_i(t)$ is $D^{\alpha}x_i(t) = \frac{1}{\Gamma(n-\alpha)}\int_{t_0}^{t}(t-\tau)^{n-\alpha-1}x_i^{(n)}(\tau)d\tau$, where $k-1 < \alpha < k \in Z^+$, $\Gamma(\cdot)$ denotes the Gamma function, $\Gamma(s) = \int_0^{\infty} t^{s-1}e^{-t}dt$, $x_i(t) \in R$, $x(t) = (x_1, x_2, \cdots, x_n)^T \in R^n$ is the n-dimensional state vector, $A \in R^{n\times n}$ stands for the linear part of the system, $f : R^n \to R^n$ represents the nonlinear part, satisfying $|f_i(x) - f_i(y)| \le \sum_{j=1}^{n} L_{ij}|x_j - y_j|, i = 1, 2, \cdots, n$, $L_{ij} > 0$. The system (1) is considered as a drive system. The slave system is given by

$$D^{\bar{\alpha}}y = Ay + f(y) + u(t), \tag{2}$$

where $y(t) \in R^n$ is the slave state vector, while $u(t)$ is the controller to be designed later.

The synchronization error is defined as the difference between the states of the master and the slave systems

$$e = y - x. \tag{3}$$

It follows from (1)–(3) that the error dynamics can be written in the following form

$$D^{\bar{\alpha}} e = Ae + f(y) - f(x) + u(t). \tag{4}$$

Our aim is to design a suitable feedback control

$$u(t) = Ke, \tag{5}$$

where $K = \text{diag}(k_1, k_2, \cdots, k_n)$, such that the following error dynamical system

$$D^{\bar{\alpha}} e = (A + K)e + f(y) - f(x), \tag{6}$$

or

$$D^{\alpha_i} e_i = \sum_{j=1}^{n} a_{ij} e_j + k_i e_i + f_i(y) - f_i(x), \;\; i = 1, 2, \cdots, n \tag{7}$$

is asymptotically stable, which implies that the trajectory of the slave IFO chaotic system (2), with initial condition $y(0)$, can asymptotically approach the drive system (1), with initial condition $x(0)$

$$\lim_{t\to\infty} \|e\| = \lim_{t\to\infty} \|x - y\| = 0. \tag{8}$$

To this end, the following lemmas and assumption need to be introduced.

Define $V(t, x(t)) = \sum_{i=1}^{n} V_i(t, x_i(t))$, $W(t, x(t)) = \sum_{i=1}^{n} W_i(t, x_i(t))$. Consider the following a set of FO inequalities and equations:

$$D^{\alpha_i} V_i(t, x_i(t)) \le g(V_1(t, x_1(t)), \cdots, V_n(t, x_n(t))), \tag{9}$$

where $g(\cdot) \in R$ and $V_i(t, x_i(t)) : [0, \infty) \times R \to [0, \infty)$ are continuously differentiable functions

$$D^{\alpha_i} W_i(t, x_i(t)) = g(t, W_1(x_1(t)), \cdots, W_n(t, x_n(t))), \tag{10}$$

where $W_i(t, x_i(t)) : [0, \infty) \times R \to [0, \infty)$ is assumed to be continuously differentiable functions.

We call Expressions (9) and (10) as the compared and the comparison systems, respectively. Therefore, by employing the following comparison principle, we can discuss the asymptotic stability of $V(t, x(t))$ using the asymptotic behavior of $W(t, x(t))$.

Lemma 1 ([35])**.** *Consider the following FO differential inequalities with initial conditions* $0 \le V_i(0, x_i(0)) \le W_i(0, y_i(0))$, $i = 1, 2, \cdots, n$

$$\begin{aligned} D^{\alpha_1} V_1(t, x_1(t)) &\le D^{\alpha_1} W_1(t, y_1(t)), \\ D^{\alpha_2} V_2(t, x_2(t)) &\le D^{\alpha_2} W_2(t, y_2(t)), \\ &\vdots \\ D^{\alpha_n} V_n(t, x_n(t)) &\le D^{\alpha_n} W_n(t, y_n(t)). \end{aligned}$$

If previous inequalities hold, then the following inequalities hold:

$$\begin{aligned} V_i(t, x_i(t)) &\le W_i(t, y_i(t)), \forall t > 0, \; i = 1, 2, \cdots, n, \\ V(t, x(t)) &\le W(t, y(t)), \forall t > 0, \end{aligned}$$

where V and $W : [0, \infty) \times R^n \to [0, \infty)$ are continuously differentiable functions.

Remark 1 ([35]). *The proof of Lemma 3.1 can also be obtained by the approach of the proof of fractional comparison principle [26]. When $V_i(t, x_i(t)) = V(t), W_i(t, x_i(t)) = W(t)$ and $V(0) = W(0)$, then Lemma 3.1 reduces to the fractional comparison principle [26].*

Lemma 2 ([36]). *The FO multi-order system $D^{\bar{\alpha}}x(t) = A_0x(t)$ is stable if there exist symmetric positive definite matrices $P_i \in H_+^{t_i\times t_i}$, $i = 1, 2, \cdots, k$ and a matrix $H \in R^{n\times n}$, such that:*

$$M + \mathrm{sym}\left\{\left(\begin{bmatrix} I_n \\ -A_0 \end{bmatrix} \otimes I_2\right)(H \otimes I_2)\left(\begin{bmatrix} I_n & I_n \end{bmatrix} \otimes I_2\right)\right\} < 0,$$

where

$$\begin{aligned} M &= \begin{bmatrix} 0_{2n\times 2n} & \oplus_{i=1}^{k}(P_i \otimes R_{\alpha_i}) \\ \oplus_{i=1}^{k}(P_i \otimes R_{\alpha_i}) & 0_{2n\times 2n} \end{bmatrix} \\ R_\alpha &= \begin{bmatrix} \sin(\frac{\alpha\pi}{2}) & \cos(\frac{\alpha\pi}{2}) \\ -\cos(\frac{\alpha\pi}{2}) & \sin(\frac{\alpha\pi}{2}) \end{bmatrix}. \end{aligned}$$

Lemma 3 ([36]). *The FO multi-order system $D^{\bar{\alpha}}x(t) = A_0x(t) + B_0u(t)$ is stabilizable under the state feedback controller $u(t) = Kx(t)$ if there exist symmetric positive definite matrices $P_i \in H_+^{t_i\times t_i}, i = 1, 2, \cdots, k$, the matrices $H \in R^{n\times n}$ and $Q \in R^{p\times n}$ such that:*

$$\begin{aligned} M + \mathrm{sym}&\left\{\left(\begin{bmatrix} I_n \\ -A_0 \end{bmatrix} \otimes I_2\right)(H \otimes I_2)\left(\begin{bmatrix} I_n & I_n \end{bmatrix} \otimes I_2\right)\right\} \\ &+ \mathrm{sym}\left\{\left(\begin{bmatrix} 0_{n\times p} \\ -B_0 \end{bmatrix} \otimes I_2\right)(Q \otimes I_2)\left(\begin{bmatrix} I_n & I_n \end{bmatrix} \otimes I_2\right)\right\} < 0. \end{aligned}$$

Moreover, the controller feedback gain is given by $K = QH^{-1}$.

Lemma 4 ([37]). *Let $x(t) \in R^n$ be a differentiable vector-value function. Then, for any time instant $t \geq t_0$*

$$D^\alpha(x^T(t)Px(t)) \leq (x^T(t)P)D^\alpha x(t) + (D^\alpha x(t))^T Px(t),$$

where $P > 0$ and $\alpha \in (0, 1)$.

3. Main Results

Theorem 1. *If there exist matrices $P_i \in H_+^{t_i\times t_i}, i = 1, 2, \cdots, k$, and diagonal matrices $H \in H^{n\times n}$ and $Q \in H^{n\times n}$ such that*

$$\begin{aligned} M + \mathrm{sym}&\left\{\left(\begin{bmatrix} I_n \\ -\tilde{A} \end{bmatrix} \otimes I_2\right)(H \otimes I_2)\left(\begin{bmatrix} I_n & I_n \end{bmatrix} \otimes I_2\right)\right\} \\ &+ \mathrm{sym}\left\{\left(\begin{bmatrix} 0_{n\times n} \\ -B \end{bmatrix} \otimes I_2\right)(Q \otimes I_2)\left(\begin{bmatrix} I_n & I_n \end{bmatrix} \otimes I_2\right)\right\} < 0, \end{aligned} \tag{11}$$

where $\tilde{A} = (\tilde{a}_{ij})_{n\times n}$, $\tilde{a}_{ii} = 2a_{ii} + 2L_{ii} + \sum_{j=1,i\neq j}^{n}(|a_{ij}| + L_{ij})$, $\tilde{a}_{ij} = \sum_{j=1}^{n}(|a_{ij}| + L_{ij})(i = 1, 2, \cdots, n, i \neq j)$, and $B = 2I$, then the drive system (1) synchronizes the corresponding response system (2). Moreover, the controller feedback gain is given by $K = QH^{-1}$.

Proof. Select the auxiliary function:

$$V(t) = \sum_{i=1}^{n} V_i(t) = \sum_{i=1}^{n} e_i^2(t).$$

Using Lemma 4 and calculating the α_i-order derivative on V_i, we obtain

$$
\begin{aligned}
D^{\alpha_1}V_1(t) &\le 2e_1(t)D^{\alpha_1}e_1(t) \\
&= 2e_1(t)\big(\sum_{j=1}^{n} a_{1j}e_j + k_1e_1 + f_1(y) - f_1(x)\big) \\
&\le \big(2a_{11} + 2L_{11} + \sum_{j=2}^{n}(|a_{1j}| + L_{1j}) + 2k_1\big)e_1^2 \\
&+ \sum_{j=2}^{n}(|a_{1j}| + L_{1j})e_j^2 \\
&= \big(2a_{11} + 2L_{11} + \sum_{j=2}^{n}(|a_{1j}| + L_{1j}) + 2k_1\big)V_1(t) \\
&+ \sum_{j=2}^{n}(|a_{1j}| + L_{1j})V_j(t), \\
D^{\alpha_2}V_2(t) &\le 2e_2(t)D^{\alpha_2}e_2(t) \\
&= 2e_2(t)\big(\sum_{j=1}^{n} a_{2j}e_j + k_2e_2 + f_2(y) - f_2(x)\big) \\
&\le \big(2a_{22} + 2L_{22} + \sum_{j=1,j\neq 2}^{n}(|a_{2j}| + L_{2j}) + 2k_2\big)e_2^2 \\
&+ \sum_{j=1,j\neq 2}^{n}(|a_{2j}| + L_{2j})e_j^2 \\
&= \big(2a_{22} + 2L_{22} + \sum_{j=1,j\neq 2}^{n}(|a_{2j}| + L_{2j}) + 2k_2\big)V_2(t) \\
&+ \sum_{j=1,j\neq 2}^{n}(|a_{2j}| + L_{2j})V_j(t), \\
&\vdots \\
D^{\alpha_n}V_n(t) &\le 2e_n(t)D^{\alpha_n}e_n(t) \\
&= 2e_n(t)\big(\sum_{j=1}^{n} a_{nj}e_j + k_ne_n + f_n(y) - f_n(x)\big) \\
&\le \big(2a_{nn} + 2L_{nn} + \sum_{j=1}^{n-1}(|a_{nj}| + L_{nj}) + 2k_n\big)e_n^2 \\
&+ \sum_{j=1}^{n-1}(|a_{nj}| + L_{nj})e_j^2 \\
&= \big(2a_{nn} + 2L_{nn} + \sum_{j=1}^{n-1}(|a_{nj}| + L_{nj} + 2k_n)\big)V_n(t) \\
&+ \sum_{j=1}^{n-1}(|a_{nj}| + L_{nj})V_j(t).
\end{aligned} \tag{12}
$$

From (12), we can construct the corresponding comparative system,

$$
\begin{bmatrix} D^{\alpha_1}W_1(t) \\ D^{\alpha_2}W_2(t) \\ \vdots \\ D^{\alpha_n}W_n(t) \end{bmatrix} = \begin{bmatrix} \bar{a}_{11} & \bar{a}_{12} & \cdots & \bar{a}_{1n} \\ \bar{a}_{21} & \bar{a}_{22} & \cdots & \bar{a}_{2n} \\ \vdots & \vdots & \ddots & \vdots \\ \bar{a}_{n1} & \bar{a}_{n1} & \cdots & \bar{a}_{3n} \end{bmatrix} \begin{bmatrix} W_1(t) \\ W_2(t) \\ \vdots \\ W_n(t) \end{bmatrix}, \tag{13}
$$

where

$$\begin{aligned}\bar{a}_{ii} &= 2a_{ii} + 2L_{ii} + \sum_{j=1, i\neq j}^{n} (|a_{ij}| + L_{ij}) + 2k_i, \\ \bar{a}_{ij} &= \sum_{j=1}^{n} (|a_{ij}| + L_{ij})(i = 1, 2, \cdots, n, i \neq j).\end{aligned}$$

System (13) can be rewritten as

$$D^{\alpha} W(t) = \tilde{A} W(t) + B\bar{K} W(t) = \tilde{A} W(t) + Bu(t), \tag{14}$$

where $W(t) = (W_1(t), W_2(t), \cdots, W_n(t))^T$, $\tilde{A} = (\tilde{a}_{ij})_{n\times n}$, $\tilde{a}_{ii} = \bar{a}_{ii} - 2k_i$, and $\tilde{a}_{ij} = \bar{a}_{ij}(i = 1, 2, \cdots, n, i \neq j)$. Compared (14) with $D^{\bar{\alpha}} x(t) = A_0 x(t) + B_0 u(t)$, let us denote $\tilde{A}$ as A_0, and $B = \mathrm{diag}(2, 2, \cdots, 2)$ as B_0 in Lemma 3. It follows from Lemma 3 that the controlled system (14) with $u = QH^{-1}W(t)$ is asymptotically stable if the appropriate condition is satisfied, meaning $W(t) \to 0$. Based on the comparison principle of FO systems with multi-order, we have $V(t) \le W(t)$ and $V(t) \to 0$. In view of $V(t) = \sum_{i=1}^{n} V_i(t) = \sum_{i=1}^{n} e_i^2(t)$, one has $e_i(t) \to 0$. Therefore, the synchronization error system (8) is also stable. This is ending the proof. □

Remark 2. *Compared to existing results [12–24], herein the fractional derivative orders of every state are assumed non-identical, which makes the synchronization control design more challenging. To cope with non-identical fractional derivative orders, the comparison principle of fractional systems with multi-order is used adopted.*

Remark 3. *Our controller is very simple and easy to implement. Moreover, the proposed method is still valid for the synchronization of IFO systems with irrational order, which a very limited number of papers have been concern on.*

4. Applications

Two illustrative examples are presented. The synchronization of the IFO Genesio-Tesi system and the IFO Hopfield neural chaotic network, to demonstrate the effectiveness of the proposed control scheme.

Example 1. *The IFO Genesio-Tesi chaotic system is described by*

$$\begin{cases} D^{\alpha_1} x_1 = x_2, \\ D^{\alpha_2} x_2 = x_3, \\ D^{\alpha_3} x_3 = -ax_1 - bx_2 - cx_3 + mx_1^2, \end{cases} \tag{15}$$

where $a = 6$, $b = 2.92$, $c = 1.2$, $m = 1$, $\alpha_1 = 0.93$, $\alpha_2 = 0.94$ and $\alpha_3 = 0.95$. A chaotic attractor is observed as shown in Figure 1. Based on the boundedness of chaotic systems and the phase space diagram, one can observe $L_{31} = 6$. Let the system (15) be the master, and the slave system be given by

$$\begin{cases} D^{\alpha_1} y_1 = y_2 + u_1, \\ D^{\alpha_2} y_2 = y_3 + u_2, \\ D^{\alpha_3} y_3 = -ay_1 - by_2 - cy_3 + my_1^2 + u_3. \end{cases} \tag{16}$$

Let the state errors be $e_1 = y_1 - x_1; e_2 = y_2 - x_2; e_3 = y_3 - x_3$, and design $u_i = k_i e_i$, $i = 1, 2, 3$. Then the error dynamics is

$$\begin{cases} D^{\alpha_1} e_1 = e_2 + k_1 e_1, \\ D^{\alpha_2} e_2 = e_3 + k_2 e_2, \\ D^{\alpha_3} e_3 = -ae_1 - be_2 - ce_3 + my_1^2 - mx_1^2 + k_3 e_3. \end{cases}$$

By a calculation, one can get

$$\tilde{A} = \begin{bmatrix} 1 & 0 & 0 \\ 0 & 1 & 0 \\ 11 & 2.92 & 12.52 \end{bmatrix}.$$

Using the LMI toolbox provided by Matlab, a feasible solution of a LMI condition (11) is obtained as follows:

$$H = \begin{bmatrix} -0.0264 & 0 & 0 \\ 0 & -0.3269 & 0 \\ 0 & 0 & -0.3284 \end{bmatrix}, Q = \begin{bmatrix} 0.4241 & 0 & 0 \\ 0 & 1.1348 & 0 \\ 0 & 0 & 1.1326 \end{bmatrix}$$

Synchronization state-feedback gain is given by

$$K = HQ^{-1} = \begin{bmatrix} -37.4819 & 0 & 0 \\ 0 & -3.3553 & 0 \\ 0 & 0 & -6.6823 \end{bmatrix}.$$

In this simulation, the initial states of the drive and response systems are $x(0) = (0.1, 0.2, 0.3)^T$ *and* $y(0) = (0.4, 0.5, 0.6)^T$*. The drive and response systems (15) and (16) are asymptotically synchronized as shown in Figure 2, synchronization error is depicted in Figure 3.*

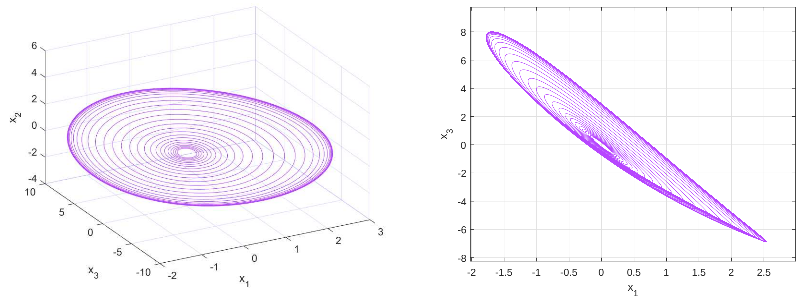

(**a**) (**b**)

Figure 1. Phase portraits of: (**a**) Chaotic attractors on $x_1 - x_2 - x_3$; (**b**) Projection of chaotic attractors on $x_1 - x_3$.

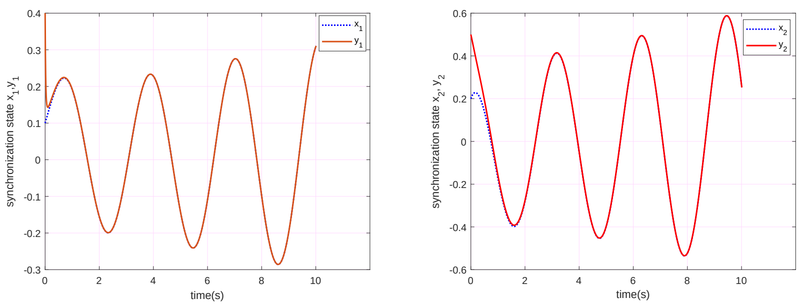

(**a**) (**b**)

Figure 2. *Cont.*

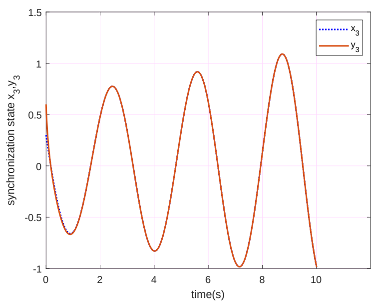

(**c**)

Figure 2. State trajectories of drive and slave systems in Example 1: (**a**) x_1 v.s. y_1, (**b**) x_2 v.s. y_2, (**c**) x_3 v.s. y_3.

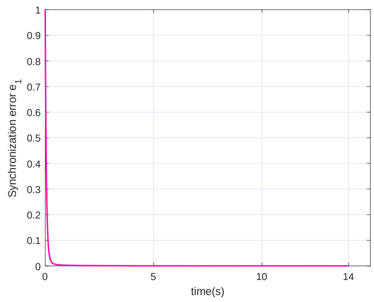

(**a**)

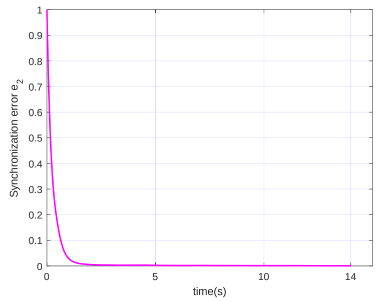

(**b**)

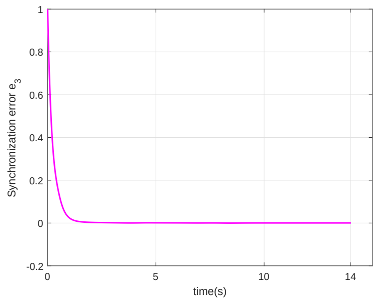

(**c**)

Figure 3. Synchronization error of drive and slave systems in Example 1: (**a**) $x_1 - y_1$, (**b**) $x_2 - y_2$, (**c**) $x_3 - y_3$.

Example 2. *The drive system is the IFO Hopfield neural chaotic network with there neurons [38]:*

$$\begin{cases} D^{\alpha_1}x_1(t) = -x_1(t) + 2\tanh(x_1(t)) - 1.2\tanh(x_2(t)), \\ D^{\alpha_2}x_2(t) = -x_2(t) + 2\tanh(x_1(t)) + 1.71\tanh(x_2(t)) + 1.15\tanh(x_3(t)), \\ D^{\alpha_3}x_3(t) = -x_3(t) - 4.75\tanh(x_1(t)) + 1.1\tanh(x_3(t)). \end{cases} \tag{17}$$

The slave system is:

$$\begin{cases} D^{\alpha_1}x_1(t) = -x_1(t) + 2\tanh(x_1(t)) - 1.2\tanh(x_2(t)) + u_1, \\ D^{\alpha_2}x_2(t) = -x_2(t) + 2\tanh(x_1(t)) + 1.71\tanh(x_2(t)) + 1.15\tanh(x_3(t)) + u_2, \\ D^{\alpha_3}x_3(t) = -x_3(t) - 4.75\tanh(x_1(t)) + 1.1\tanh(x_3(t)) + u_3. \end{cases} \tag{18}$$

From (17), one can obtain $L_{11} = L_{21} = 2, L_{12} = 1.2, L_{13} = 0, L_{22} = 1.71, L_{23} = 1.15, L_{31} = 4.75, L_{32} = 0$ and $L_{33} = 1.1$. As shown in Figure 4, the IFO Hopfield neural network (18) possesses chaotic behavior when $\alpha_1 = 0.96$, $\alpha_2 = 0.97$, and $\alpha_3 = 0.98$. It follows from (17) and (18) that one can obtain

$$\tilde{A} = \begin{bmatrix} 3.2 & 1.2 & 0 \\ 2.1 & 4.57 & 1.15 \\ 4.75 & 0 & 4.95 \end{bmatrix}.$$

Using the Matlab LMI toolbox, it is straightforward to find that the linear matrix inequality (11) in Theorem 1 is feasible, which implies that the error system is asymptotically stable, and a feasible solution of an LMI condition (11) is described as:

$$H = \begin{bmatrix} -0.0259 & 0 & 0 \\ 0 & -0.3364 & 0 \\ 0 & 0 & -1.3999 \end{bmatrix}, Q = \begin{bmatrix} 0.9706 & 0 & 0 \\ 0 & 1.1286 & 0 \\ 0 & 0 & 9.3542 \end{bmatrix},$$

with the synchronization state-feedback gain given by

$$K = HQ^{-1} = \begin{bmatrix} -16.0568 & 0 & 0 \\ 0 & -3.4715 & 0 \\ 0 & 0 & -3.4483 \end{bmatrix}.$$

According to Theorem 1, the synchronization between (17) and (18) can be achieved. In the numerical simulations, the initial states of the drive and response systems are taken as $x(0) = (3,1,2)^T$ and $y(0) = (4,2,3)^T$, respectively. Figure 5 shows the state synchronization trajectory of the drive and response systems. Figure 6 depicts the synchronization error.

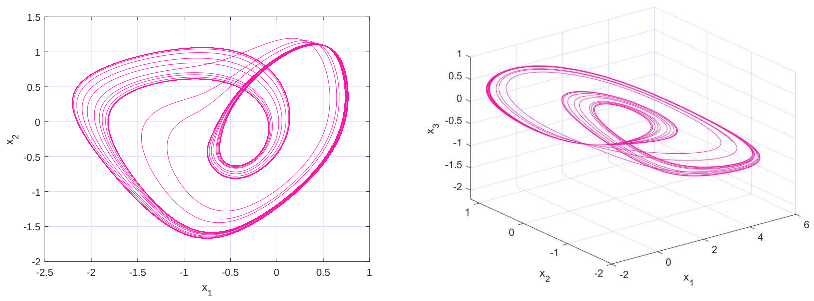

(**a**) (**b**)

Figure 4. Phase portraits of: (**a**) Projection of chaotic attractors on $x_1 - x_2$; (**b**) Chaotic attractors on $x_1 - x_2 - x_3$.

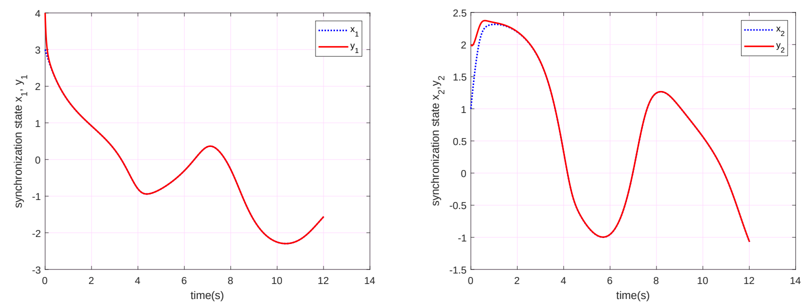

(**a**) (**b**)

Figure 5. *Cont.*

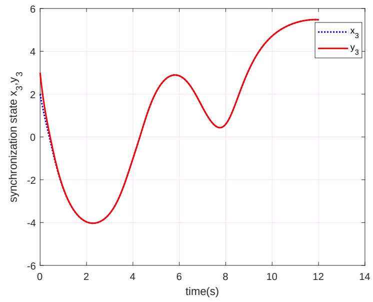

(**c**)

Figure 5. State trajectories of the drive and slave systems in Example 2: (**a**) x_1 v.s. y_1, (**b**) x_2 v.s. y_2, (**c**) x_3 v.s. y_3.

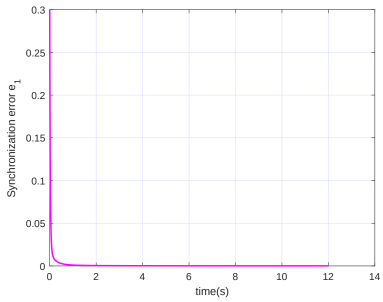

(**a**)

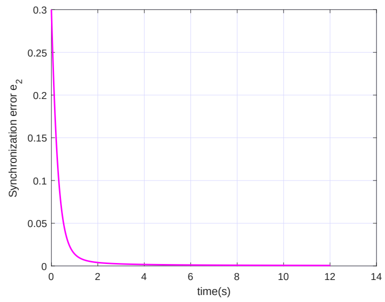

(**b**)

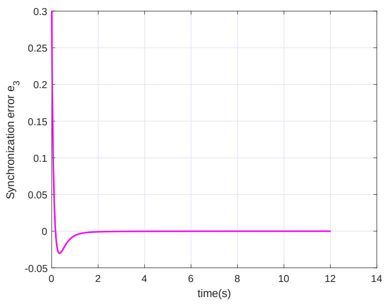

(**c**)

Figure 6. Synchronization error of the drive and slave systems in Example 2: (**a**) $x_1 - y_1$, (**b**) $x_2 - y_2$, (**c**) $x_3 - y_3$.

5. Conclusions

This paper investigated the synchronization of IFO chaotic systems. Based on the LMI approach and comparison principle of fractional systems with multi-order, a linear feedback control design method was proposed. The method tends to be simple, economical and easy to realize, and being also valid for IFO chaotic systems with irrational order. The feasibility and effectiveness of the approach was verified by means of two numerical examples. The synchronization of fractional variable order systems will become a relevant topic in the near future, since it was shown that chaotic behavior can also exist in such kind of systems. This will be addressed in our further research.

Author Contributions: Methodology, F.Q.; software, L.C.; validation and data curation, Y.C.; writing—original draft preparation, F.Q.; writing—review and editing, A.M.L.; supervision and project administration, J.Q. All authors have read and agreed to the published version of the manuscript.

Funding: This work was supported by the National Natural Science Funds of China (Nos. 61633005; 62073114; 11971032) and National Key R& D Program of China (No. 2020YFB2009400).

Institutional Review Board Statement: Not applicable.

Informed Consent Statement: Not applicable.

Data Availability Statement: Not applicable.

Conflicts of Interest: The authors declare no conflict of interest.

References

1. Xue, D. *Fractional-Order Control Systems*; de Gruyter: Berlin, Germany, 2017.
2. Hilfer, R. *Applications of Fractional Calculus in Physics*; World Scientific: Singapore, 2000.
3. Chen, W.; Sun, H.; Li, X. *Fractional Derivative Modeling in Mechanics and Engineering*; Springer: Berlin/Heidelberg, Germany, 2010.
4. Anastassiou, G.A. *Generalized Fractional Calculus: New Advancements and Applications*; Springer Nature: Berlin/Heidelberg, Germany, 2020; Volume 305.
5. Petráš, I. *Fractional-Order Nonlinear Systems: Modeling, Analysis and Simulation*; Springer Science & Business Media: Berlin/Heidelberg, Germany, 2011.
6. Tarasov, V.E.; Tarasova, V.V. *Economic Dynamics with Memory: Fractional Calculus Approach*; Walter de Gruyter GmbH & Co. KG: Berlin, Germany, 2021; Volume 8.
7. Hartley, T.T.; Lorenzo, C.F.; Qammer, H.K. Chaos in a fractional order Chua's system. *IEEE Trans. Circ. Syst. Fundam. Theory Appl.* **1995**, *42*, 485–490. [CrossRef]
8. Deshpande, A.S.; Daftardar-Gejji, V.; Sukale, Y.V. On Hopf bifurcation in fractional dynamical systems. *Chaos Solitons Fractals* **2017**, *98*, 189–198. [CrossRef]
9. Huang, C.; Li, H.; Cao, J. A novel strategy of bifurcation control for a delayed fractional predator—Prey model. *Appl. Math. Comput.* **2019**, *347*, 808–838. [CrossRef]
10. Chen, L.; Yin, H.; Huang, T.; Yuan, L.; Zheng, S.; Yin, L. Chaos in fractional-order discrete neural networks with application to image encryption. *Neural Netw.* **2020**, *125*, 174–184. [CrossRef] [PubMed]
11. Kamal, F.; Elsonbaty, A.; Elsaid, A. A novel fractional nonautonomous chaotic circuit model and its application to image encryption. *Chaos Solitons Fractals* **2021**, *144*, 110686. [CrossRef]
12. Tavazoei, M.S.; Haeri, M. Synchronization of chaotic fractional-order systems via active sliding mode controller. *Phys. Stat. Mech. Its Appl.* **2008**, *387*, 57–70. [CrossRef]
13. Akgül, A.; Rajagopal, K.; Durdu, A.; Pala, M.A.; Boyraz, Ö.F.; Yildiz, M.Z. A simple fractional-order chaotic system based on memristor and memcapacitor and its synchronization application. *Chaos Solitons Fractals* **2021**, *152*, 111306. [CrossRef]
14. Bhalekar, S.; Daftardar-Gejji, V. Synchronization of different fractional order chaotic systems using active control. *Commun. Nonlinear Sci. Numer. Simul.* **2010**, *15*, 3536–3546. [CrossRef]
15. Wang, F.; Zheng, Z.; Yang, Y. Quasi-synchronization of heterogenous fractional-order dynamical networks with time-varying delay via distributed impulsive control. *Chaos Solitons Fractals* **2021**, *142*, 110465. [CrossRef]
16. Aadhithiyan, S.; Raja, R.; Zhu, Q.; Alzabut, J.; Niezabitowski, M.; Lim, C. Modified projective synchronization of distributive fractional order complex dynamic networks with model uncertainty via adaptive control. *Chaos Solitons Fractals* **2021**, *147*, 110853. [CrossRef]
17. Zambrano-Serrano, E.; Bekiros, S.; Platas-Garza, M.A.; Posadas-Castillo, C.; Agarwal, P.; Jahanshahi, H.; Aly, A.A. On chaos and projective synchronization of a fractional difference map with no equilibria using a fuzzy-based state feedback control. *Phys. Stat. Mech. Its Appl.* **2021**, *578*, 126100. [CrossRef]
18. Wu, C.J.; Zhang, Y.B.; Yang, N.N. The synchronization of a fractional order hyperchaotic system based on passive control. *Chin. Phys.* **2011**, *20*, 060505. [CrossRef]
19. Chen, Y.; Tang, C.; Roohi, M. Design of a model-free adaptive sliding mode control to synchronize chaotic fractional-order systems with input saturation: An application in secure communications. *J. Frankl. Inst.* **2021**, *358*, 8109–8137. [CrossRef]
20. Zhang, K.; Wang, H.; Fang, H. Feedback control and hybrid projective synchronization of a fractional-order Newton–Leipnik system. *Commun. Nonlinear Sci. Numer. Simul.* **2012**, *17*, 317–328. [CrossRef]
21. Razminia, A.; Baleanu, D. Complete synchronization of commensurate fractional order chaotic systems using sliding mode control. *Mechatronics* **2013**, *23*, 873–879. [CrossRef]
22. Yu, J.; Hu, C.; Jiang, H.; Fan, X. Projective synchronization for fractional neural networks. *Neural Netw.* **2014**, *49*, 87–95. [CrossRef]
23. Chen, L.; Chai, Y.; Wu, R. Lag projective synchronization in fractional-order chaotic (hyperchaotic) systems. *Phys. Lett. A* **2011**, *375*, 2099–2110. [CrossRef]
24. Zhang, W.; Cao, J.; Wu, R.; Alsaadi, F.E.; Alsaedi, A. Lag projective synchronization of fractional-order delayed chaotic systems. *J. Frankl. Inst.* **2019**, *356*, 1522–1534. [CrossRef]
25. Matignon, D. *Stability Properties for Generalized Fractional Differential Systems*; ESAIM: Proceedings; EDP Sciences: Les Ulis, France, 1998; Volume 5, pp. 145–158.
26. Li, Y.; Chen, Y.; Podlubny, I. Stability of fractional-order nonlinear dynamic systems: Lyapunov direct method and generalized Mittag–Leffler stability. *Comput. Math. Appl.* **2010**, *59*, 1810–1821. [CrossRef]

27. Tavazoei, M.S.; Haeri, M. Chaotic attractors in incommensurate fractional order systems. *Phys. Nonlinear Phenom.* **2008**, *237*, 2628–2637. [CrossRef]
28. Ma, C.; Mou, J.; Liu, J.; Yang, F.; Yan, H.; Zhao, X. Coexistence of multiple attractors for an incommensurate fractional-order chaotic system. *Eur. Phys. J. Plus* **2020**, *135*, 1–21. [CrossRef]
29. Huang, C.; Cao, J.; Xiao, M.; Alsaedi, A.; Alsaadi, F.E. Controlling bifurcation in a delayed fractional predator–prey system with incommensurate orders. *Appl. Math. Comput.* **2017**, *293*, 293–310. [CrossRef]
30. Debbouche, N.; Almatroud, A.O.; Ouannas, A.; Batiha, I.M. Chaos and coexisting attractors in glucose-insulin regulatory system with incommensurate fractional-order derivatives. *Chaos Solitons Fractals* **2021**, *143*, 110575. [CrossRef]
31. Zouari, F.; Boulkroune, A.; Ibeas, A. Neural adaptive quantized output-feedback control-based synchronization of uncertain time-delay incommensurate fractional-order chaotic systems with input nonlinearities. *Neurocomputing* **2017**, *237*, 200–225. [CrossRef]
32. Boulkroune, A.; Bouzeriba, A.; Bouden, T. Fuzzy generalized projective synchronization of incommensurate fractional-order chaotic systems. *Neurocomputing* **2016**, *173*, 606–614. [CrossRef]
33. Martínez-Guerra, R.; Pérez-Pinacho, C.A.; Gómez-Cortés, G.C. An Observer for a Class of Incommensurate Fractional-Order Systems. In *Synchronization of Integral and Fractional Order Chaotic Systems*; Springer: Berlin/Heidelberg, Germany, 2015; pp. 219–236.
34. Zhou, Y.; Liu, H.; Cao, J.; Li, S. Composite learning fuzzy synchronization for incommensurate fractional-order chaotic systems with time-varying delays. *Int. J. Adapt. Control. Signal Process.* **2019**, *33*, 1739–1758. [CrossRef]
35. Lenka, B.K. Fractional comparison method and asymptotic stability results for multivariable fractional order systems. *Commun. Nonlinear Sci. Numer. Simul.* **2019**, *69*, 398–415. [CrossRef]
36. Lu, J.G.; Zhu, Z.; Ma, Y.D. Robust stability and stabilization of multi-order fractional-order systems with interval uncertainties: An LMI approach. *Int. J. Robust Nonlinear Control.* **2021**, *31*, 4081–4099. [CrossRef]
37. Liang, S.; Wu, R.; Chen, L. Adaptive pinning synchronization in fractional-order uncertain complex dynamical networks with delay. *Phys. Stat. Mech. Its Appl.* **2016**, *444*, 49–62. [CrossRef]
38. Chen, L.; Qu, J.; Chai, Y.; Wu, R.; Qi, G. Synchronization of a class of fractional-order chaotic neural networks. *Entropy* **2013**, *15*, 3265–3276. [CrossRef]